[1] J. Stubbe, W. A. van der Donk, *Chem. Rev.* **1998**, *98*, 705 – 762.
[2] J. Rétey, *Angew. Chem.* **1990**, *102*, 373 – 379; *Angew. Chem. Int. Ed. Engl.* **1990**, *29*, 355 – 361.
[3] *Vitamin B_{12} and B_{12}-Proteins* (Eds.: B. Kräutler, D. Arigoni, B. T. Golding), Wiley-VCH, Weinheim, **1998**.
[4] J. Halpern, *Science* **1985**, *227*, 869 – 875.
[5] S. Licht, G. J. Gerfen, J. Stubbe, *Science* **1996**, *271*, 477 – 481.
[6] B. T. Golding, R. J. Anderson, S. Ashwell, C. H. Edwards, I. Garnett, F. Kroll, W. Buckel in *Vitamin B_{12} and B_{12}-Proteins* (Eds.: B. Kräutler, D. Arigoni, B. T. Golding), Wiley-VCH, Weinheim, **1998**, pp. 201 – 216.
[7] F. Mancia, N. H. Keep, A. Nakagawa, P. F. Leadlay, S. McSweeney, B. Rasmussen, P. Bosecke, O. Diat, P. R. Evans, *Structure* **1996**, *4*, 339 – 350.
[8] F. Mancia, P. R. Evans, *Structure* **1998**, *6*, 711 – 720.
[9] R. Reitzer, K. Gruber, G. Jogl, U. G. Wagner, H. Bothe, W. Buckel, C. Kratky, *Structure* **1999**, *7*, 891 – 902.
[10] N. Shibata, J. Masuda, T. Tobimatsu, T. Toraya, K. Suto, Y. Morimoto, N. Yasuoka, *Structure* **1999**, *7*, 997 – 1008.
[11] H. Bothe, D. J. Darley, S. P. J. Albracht, G. J. Gerfen, B. T. Golding, W. Buckel, *Biochemistry* **1998**, *37*, 4105 – 4113.
[12] G. J. Gerfen in *Chemistry and Biochemistry of B_{12}* (Ed.: R. Banerjee), Wiley, New York, **1999**, pp. 165 – 195.
[13] G. J. Gerfen, S. Licht, J. P. Willems, B. M. Hoffman, J. Stubbe, *J. Am. Chem. Soc.* **1996**, *118*, 8192 – 8197.
[14] E. N. G. Marsh, D. P. Ballou, *Biochemistry* **1998**, *37*, 11 864 – 11 872.
[15] R. Padmakumar, R. Padmakumar, R. Banerjee, *Biochemistry* **1997**, *36*, 3713 – 3718.
[16] a) Glutamate mutase is known to lose its activity in the presence of substrate within several hours with concomitant formation of protein-bound cob(II)alamin.[16b] It is not known whether this inactivation also occurred under the crystallization conditions (see Experimental Section). In any case, there is no doubt that the two species (A and B) are structurally related to reaction intermediates b and c of Scheme 2. b) O. Zelder, B. Beatrix, U. Leutbecher, W. Buckel, *Eur. J. Biochem.* **1994**, *226*, 577 – 585.
[17] a) M. Levitt, A. Warshel, *J. Am. Chem. Soc.* **1978**, *100*, 2607 – 2613; b) K. A. Brameld, W. A. Goddard III, *J. Am. Chem. Soc.* **1999**, *121*, 985 – 993.
[18] F. Mancia, G. A. Smith, P. R. Evans, *Biochemistry* **1999**, *38*, 7999 – 8005.
[19] a) In B_{12} dependent ribonucleotide reductases, EPR data[13] yielded a distance between the cobalt center and the radical mediator of around 8 Å, in the same range as the cobalt – substrate distance in Glm. For diol dehydratase, the substrate has a different position relative to the cofactor,[10] and rotation about the glycosidic bond has been proposed for radical transport.[19b] b) J. Masuda, N. Shibata, Y. Morimoto, T. Toraya, N. Yasuoka, *Structure* **2000**, *8*, 775 – 788.
[20] Z. Otwinowski, W. Minor, *Methods Enzymol.* **1997**, *276*, 307 – 326.
[21] G. M. Sheldrick, SHELXL-97, a program for the refinement of crystal structures from diffraction data, University of Göttingen, Göttingen, **1997**.
[22] G. J. Kleywegt, A. T. Brunger, *Structure* **1996**, *4*, 897 – 904.
[23] P. J. Kraulis, *J. Appl. Crystallogr.* **1991**, *24*, 946 – 950.
[24] E. A. Merritt, D. J. Bacon, *Methods Enzymol.* **1997**, *277*, 505 – 524.

"Carving on the Nanoscale": Polymers for the Site-Specific Dissolution of Calcium Phosphate**

Anna Peytcheva and Markus Antonietti*

In biologically mineralized systems the constructive interaction of the inorganic crystal phase with the organic matrix material results in composite materials that are exceptional in their outward appearance and material properties.[1, 2] Of the 60 minerals known to be "processed" by living organisms, the most frequently used are calcium carbonate, calcium phosphate, and hydrous silica. They are used for the formation of scales, prickles, shells, or endoskeletons. The mineral is usually crystallized within a protein or polysaccharide matrix which has a number of functions: it shapes and aligns the single-crystalline building blocks, and it serves as a ductile component for mechanical stress dissipation.[3, 4] The resulting nanoscale composite structures make biominerals such as bone or teeth superior to most artificial ceramics.

One of the reoccurring motives in biomineralization is that the polymer controls the crystal structure or the biomineral shape, in that the crystal surface is stabilized by an opposite, complementary form of the polymer, which results in an overall structure of minimal energy.[5, 6] This method can be described by ideas that originate from solid-state physics ("finding epitaxial relations"), but that do not consider polymer flexibility or adaptability. For simplicity, this class of models is called "energetical" models.

On the other hand, it is well known in biomedicine and colloid chemistry that crystals in equilibrium with a supporting aqueous phase are not static objects but are continuously reconstructed. Thus the crystal shape is the result of dynamic processes, that is, the crystal geometries which are built up fastest and dissolved slowest are those that survive. A model based upon interfacial energies and kinetics was introduced and improved over the years by Nancollas and Wu[7] with a special emphasis on calcium phosphates. Here, the influence of a polymer or the biomatrix is purely kinetic, the structure-controlling molecules are not necessarily bound to the surface, but act by lowering the averaged surface energy, and an epitaxial fit of polymer and crystal is not required. We call this mode of operation the "kinetic" mode.

Although important for biomedicine and for controlled nanoparticle synthesis, there is still some controversy about the validity of both mechanisms. The development of scanning force microscopy (SFM) allowed the visualization of dissolution and growth processes in water in a time-resolved fashion.[8, 9] First experiments focused on the influence of low molecular weight components such as aspartic acid[10] or magnesium ions[11] on the growth of calcium carbonate. Also

[*] Prof. Dr. M. Antonietti, Dr. A. Peytcheva
Max Planck Institute of Colloids and Interfaces
Am Mühlenberg 1, 14476 Golm (Germany)
Fax: (+49) 331-567-9502
E-mail: pape@mpikg-golm.mpg.de

[**] Financial support by the Max Planck Society is gratefully acknowledged We thank Dr. H. Cölfen, MPI Golm and Dr. H. Schnablegger, Universität Hamburg, for helpful discussions..

  1433-7851/01/4018-3380 $ 17.50+.50/0

protein fractions extracted from seashells[12] or from algae[13] have been added to growing calcite crystals so that these molecular controlling units can be observed "at work" in solution.

Herein, we focus on the biomedically relevant calcium phosphate (bone and teeth) and examine the controlled redissolution of model crystals. These crystals were grown by the double-jet technique[14] which allows a high monodispersity and structural uniformity of the particles.[15, 16] The observation of dissolution instead of crystallization is experimentally much more simple and also reproducible than crystal growth. The results of such experiments can be understood as a "structural inversion of kinetics", that is, the sites and faces being dissolved fastest will never be found exposed in a crystallization experiment, whereas the remaining faces are most favored and are also those which dominate a crystal formed under similar conditions. The platelike crystals of brushite were chosen as a good model system, since they are very stable against other structural rearrangements, sufficiently thick to be not immediately dissolved, and exhibit a smooth and even (010) plane with an area of $1-2\,mm^2$ suitable as a substrate for SFM. However, we expect that the general trends found for brushite also hold for the other calcium phosphate polymorphs.

Droplets of a solution containing crystals are allowed to dry on a freshly cleaved mica surface. On top of the mica, a fluid cell for SFM is placed. Different polymer solutions are injected through a thin capillary so that they thoroughly wet the crystal surface. Images of the dissolution of the crystal surface under the influence of the polymer solution are recorded with a scan rate of 0.5 lines per second. The digital resolution of all the pictures is 256×256 points.

The experiments were repeated on different crystals of one sample as well as with different samples to show that the single crystal behaves as the ensemble of crystals. Thus, the presented "single site" experiments represent a sufficiently averaged limit in time and scale for the kinetic–thermodynamic results to be reproducible. This is different to mechanical atomic force microscopy (AFM) experiments with single molecules.

The scanning force microscope used is a commercial Nanoscope IIIa (Digital Instruments, Santa Barbara, USA) operating in contact mode in air and in tapping mode in liquid. It was equipped with a 100×100 μm J-scanner, with commercial silicon cantilevers (NT-MDT, Moscow) used in liquid at resonance frequencies of 5–40 kHz and with a radius of curvature ≤ 10 nm.

As polymers with specific mineral interactions (as opposed to the extracted, chemically uniform, biomaterial species investigated to date), two thermally polymerized poly(sodium)aspartate samples (which have been optimized for their application as lime-scale inhibitors; Rohm & Haas)[17] with different molecular weights, as well as poly(L+)lysin and bovine serum albumin (BSA) from Sigma Chemicals were chosen.

As a reference experiment, the unspecific dissolution of the (010) plane of brushite in deionized water was examined. The SFM image in Figure 1 presents the characteristic pattern

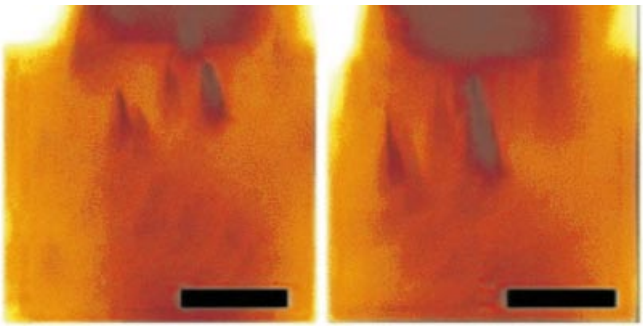

Figure 1. SFM height images of the (010) plane of brushite in deionized water, taken with a time interval of 2048 s. Scale bar = 2 μm.

which accompanies the dissolution. Triangular etch pits are framed by three characteristic steps which are parallel to the crystallographic directions (201), (001), and (101).[18] These directions coincide with partly or fully double bonded ion rows within the crystal lattice[19] (see also Figure 5). The analysis of the SFM height image shows that the (010) plane is dissolved in terraces of 7 Å height which correspond to one monolayer of the brushite crystal. This is in good agreement with data published by other authors.[9] Recording successive pictures results in a movie of the time-dependence of dissolution.[24] Form the series of images, a velocity of dissolution can be calculated which along the (201) step is estimated to $0.16\,nm\,s^{-1}$.

The same experiment was repeated in the presence of a dilute aqueous solution ($0.63\,\mu mol\,L^{-1}$) of poly(sodium)aspartate with molecular weight $18\,000\,g\,mol^{-1}$ (pH of 8.1). The SFM height images in Figure 2 are selected from a series of 24.[24] Noteworthy is that there is no polymer adsorption onto the crystal surface. This finding is in good agreement with equilibrium binding constants determined by Nancollas and Tsortos for a similar polyaspartate on the related hydroxyapatite.[20] All interactions of the polymer with the (010) plane are therefore temporary and kinetic.

The dissolution of the (010) plane follows the triangular pattern known from the experiments in deionized water.

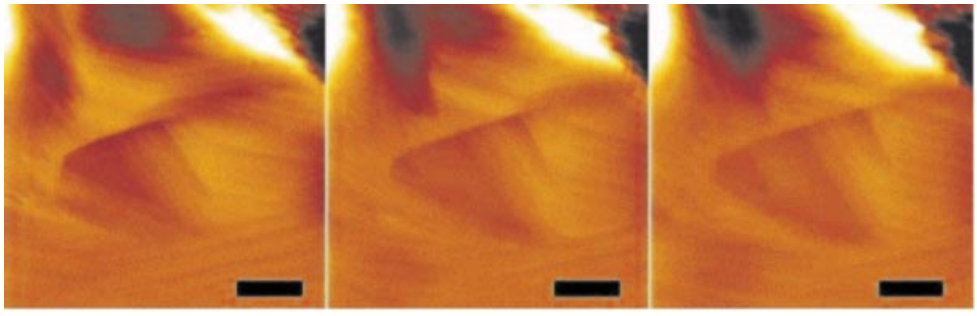

Figure 2. SFM height images of the (010) plane of brushite in $0.63\,\mu mol\,L^{-1}$ polyaspartate solution selected from a series of 24 pictures taken at 512 s intervals. Scale bar = 1 μm.

  1433-7851/01/4018-3381 $ 17.50+.50/0

Pronounced complexation of Ca^{2+} ions by the carboxylate groups of the poly(sodium)aspartate can be assumed while no flocculation of the polymer is found. However, major differences are found for the dissolution of the (010) plane of brushite in poly(sodium)aspartate compared to the dissolution in deionized water:

- The velocity of dissolution along the (201) step rises to 0.45 nm s^{-1}, that is, the complexing carboxylic acid units promote dissolution (the expected result).
- Dissolution perpendicular to the (010) plane occurs, that is, the polymer works itself into the plane of observation. In water, these planes just dissolve layer-by-layer from the side, whereas the polymer allows penetration into a bare and otherwise intact crystal plane.
- The conversion of brushite into hydroxyapatite is completely suppressed (not seen by SFM, but seen in the macroscopic crystallization experiments).

This attack of the bare crystal planes is also nicely seen by light microscopy after longer contact times with the polymer solution (Figure 3); the molecular holes seen by SFM have grown to create a typical surface texture of the crystal.

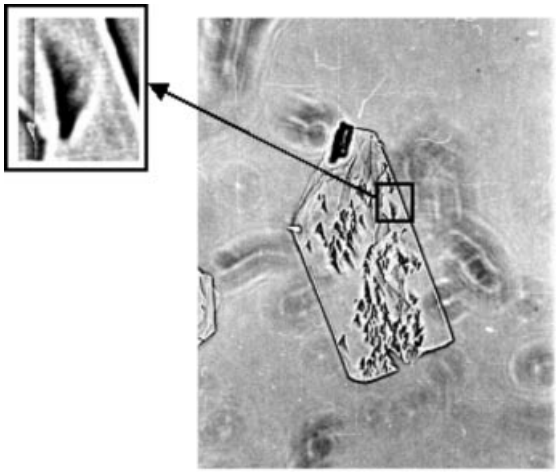

Figure 3. Light microscopy of a brushite crystal (length 0.5 mm) after contact with a polyaspartate solution of 18000 g mol^{-1} molecular weight.

The obvious question to ask is, are both the increase of the dissolution rate as well as the ability of the polymer to attack moieties in the plane really a result of the added polymer and not the result of the change of pH? Reference experiments with a low molecular weight acid or even the poly(sodium)aspartate with lower molecular weight (10000 g mol^{-1}) showed at the same molar concentration a much slower dissolution (very close to the behavior in pure water, and no considerable dissolution perpendicular to the (010) plane was detected. This is clear proof that the effect is because of the specific polymer and relies on a distinct mesoscopic size and a distinct pattern of functional groups. These observations also support the kinetic model and can be explained in that the accumulation of polymers close to attracting surfaces or the probability of contact increase with increasing polymer size and molecular weight.

Beside of the industrially relevant poly(sodium)aspartate, it is interesting to follow polypeptides throughout the regulation of mineralization/demineralization processes. In contrast to previous work we focus on the use of very simple and common model peptide structures. Albumines are an essential component of biological mineralization reactions (as shown for bone[21]). Taking into account that the known and characterized bovine serum albumine (BSA) consists of 582 amino acid residues, 41 of which are aspartic acid, 59 glutamic acid, and 59 lysine units,[22] its ability to interact with minerals becomes obvious.

Again, a BSA solution was prepared in the concentration 0.63 μmol L^{-1} at pH 5.5 and brought into contact with the (010) plane of brushite. The result of the dissolution experiment is shown in three SFM amplitude images in Figure 4 which were taken at 512 s intervals. Again no protein adsorption onto the crystal surface is observed; the protein essentially stays in solution. The triangular pits, already known from the poly(sodium)aspartate solutions, confirm that step edges along the same strongly bonded ion rows are formed as seen in Figure 1. Also, to a minor extent, dissolution from sites within the plane is observed, which we attribute to the carboxylic sites and the sufficiently high molecular weight of BSA. In addition, there is a set of new characteristic steps appearing with time, indicated with arrows in Figure 4, which were not seen in the previous dissolution experiments. Knowing the crystal structure and the orientation of the brushite crystals (fixed by the direction of the pits, which are the Ca-rich [201] and [101] edges), it is straightforward to index these newly occurring stable edges: Figure 5 shows that they are formed along directions lacking doubly bonded calcium ions in the crystal lattice. Obviously, the binding between calcium sites and the carboxyl groups of the amino acids can not account for the stabilization of these steps.

The cationic groups of BSA, mainly the 59 lysine residues, have the possibility to interact selectively with the phosphate ions of the crystal lattice. To check this hypothesis, a pure poly(L+)lysin with a molecular weight of 27000 g mol^{-1} was independently used as crystallization modifier. Since our SFM

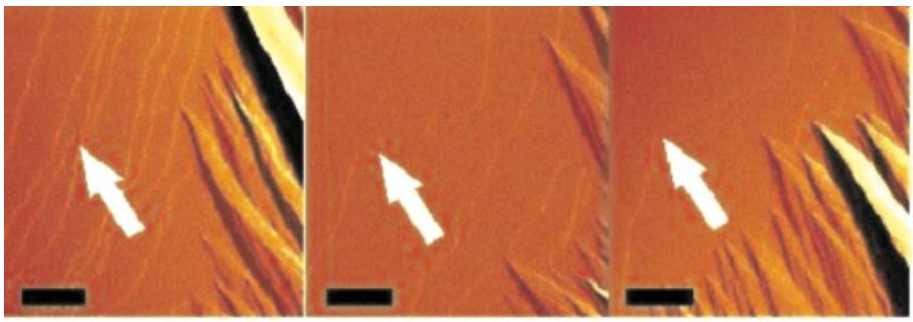

Figure 4. SFM amplitude images of the (010) plane of brushite in 0.63 μmol L^{-1} BSA solution. Scale bar = 1 μm.

  1433-7851/01/4018-3382 $ 17.50+.50/0 *Angew. Chem. Int. Ed.* **2001**, *40*, No. 18

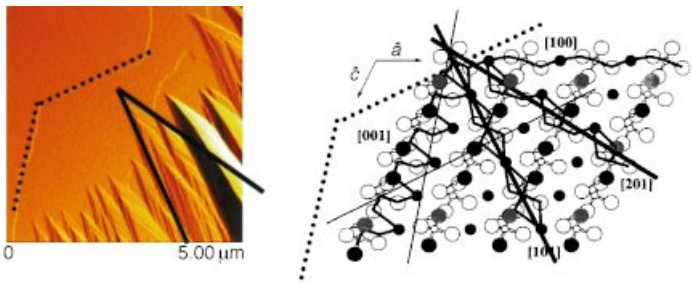

Figure 5. Assignment of the AFM image of Figure 4 to the crystallographic directions of brushite. The newly exposed edges correspond to phosphate-rich sections through the unit cell.

setup does not allow molecular resolution with cationic polyelectrolytes (they bind to the tip and most other surfaces), images of the crystals taken in a light microscope were analyzed. Figure 6 shows a brushite crystal aged for two days in a poly(L+)lysine solution.

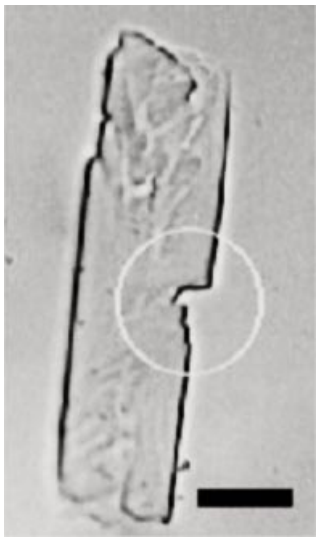

Figure 6. Light microscope image of the (010) plane of brushite in poly(L+)lysine solution. Scale bar = 200 µm.

First, it is underlined that the developing surface structures are not induced by cracking, since those structural motives develop uniformly from whole crystals in a thermo-controlled, sealed liquid cell. The pattern found also has nothing in common with the triangular pits on the crystal surface caused by poly(sodium)aspartate or BSA (anionic polymers). This reflects the obvious fact that a cationic polymer can interact with a number of faces or edges but does not stabilize those where Ca^{2+} ions are exposed. In addition, no dissolution from the surfaces, only from the edges is found, that is, the attack of intact planes is indeed specific for the polycarboxylic acids. The measured angles being exposed in these crystals (Figure 5) correspond to those of the additional step edges on the crystals aged in the BSA solution. This comparison supports the idea that these additional step edges were indeed generated by interaction promoted by the lysine moieties in the BSA.

At the low concentrations applied in our experiments, the adsorption of polymers onto the brushite (010) plane by interaction of their functional groups with the lattice ions is not observed in any experiment. Instead, a highly selective dissolution of the crystal surface takes place, which is not caused by pH changes or local functional patterns, as shown by the use of polymers with different molecular weights. Presumably the modifier accumulates close to the crystal because of partial binding and controls the surface by promoting dissolution of different sites with different selectivity. The proximity of a polymer lowers the interfacial energy of the different crystal surfaces, which gives rise to an altered dissolution and growth behavior. Our experiments agree well with the observations of Nancollas et al. who described effective blocking of crystal growth of calcium phosphate octahydrate with polyaspartic acids at a surface occupation of 1 % of the total crystal area,[23] which precludes a merely static structural explanation.

The ability to attack even the intact (010) plane is clearly a function of the molecular weight of the acidic polymer, and different functional polypeptides act as different "carving tools" exposing different crystal faces after their application. Interestingly, the rather simple and well known BSA interacts and modifies calcium phosphate by two operational modes, either employing the acidic or basic groups of the amino acids.

Clearly in our experiments kinetic considerations are more significant than epitaxial matching between the crystal lattice and the polymer. This points to a more flexible approach to the processes of controlled crystallization or dissolution by using the concept of interface energies and dynamic crystallization/dissolution equilibria.

Received: February 22, 2001
Revised: June 28, 2001 [Z16668]

[1] S. Mann in *Biomimetic Materials Chemistry* (Ed.: S. Mann), VCH, **1996**, p. 1.
[2] S. Mann in *Inorganic Materials* (Eds.: D. W. Bruce, D. O'Hare), 2nd ed., Wiley, **1996**, p. 255.
[3] S. Weiner, L. Addadi, *J. Mater. Chem.* **1997**, *7*, 689.
[4] E. Beniash, L. Addadi, S. Weiner, *J. Struct. Biol.* **1999**, *125*, 50.
[5] S. Mann, B. R. Heywood, S. Rajam, J. D. Birchall, *Nature* **1998**, *334*, 692.
[6] B. R. Heywood, S. Mann, *Adv. Mater.* **1994**, *6*, 9.
[7] G. H. Nancollas, W. J. Wu, *J. Cryst. Growth* **2000**, *11*, 137.
[8] P. E. Hillner, A. J. Gratz, S. Manne, P. K. Hansma, *Geology* **1992**, *20*, 359.
[9] P. E. Hillner, S. Manne, A. J. Gratz, P. K. Hansma, *Ultramicroscopy* **1992**, *42*, 1387.
[10] H. H. Teng, P. M. Dove, C. A. Orme, J. J. De Yoreo, *Science* **1998**, *282*, 724.
[11] K. J. Davis, P. M. Dove, J. J. De Yoreo, *Science* **2000**, *290*, 1134.
[12] D. A. Walters, B. L. Smith, A. M. Belcher, G. T. Paloczo, G. D. Stucky, D. E. Morse, P. K. Hansma, *Biophys. J.* **1997**, *72*, 1425.
[13] B. L. Smith, G. T. Paloczi, P. K. Hansma, R. P. Levine, *J. Cryst. Growth* **2000**, *211*, 116.
[14] M. Sedlak, M. Antonietti, H. Cölfen, *Macromol. Chem. Phys.* **1998**, *199*, 247.
[15] J. Stavek, M. Sipek, I. Hirasawa, K. Toyokura, *Chem. Mater.* **1996**, *4*, 545.
[16] E. Matijevic, *Curr. Opin. Colloid Interface Sci.* **1996**, *1*, 176.
[17] S. K. Wolk, G. Swift, Y. H. Paik, K. M. Yocom, R. L. Smith, E. S. Simon, *Macromolecules* **1994**, *27*, 7613.
[18] L. Scudiero, S. C. Langford, J. T. Dickinson, *Tribol. Lett.* **1999**, *6*, 41.
[19] C. A. Beevers, *Acta Chrystallogr.* **1958**, *11*, 273.
[20] A. Tsortos, G. H. Nancollas, *J. Colloid Interface Sci.* **1999**, *209*, 109.
[21] M. Owen, J. T. Triffitt, R. A. Melick in *Hard Tissue Growth, Repair and Remineralization* (Eds.: K. Elliott, D. W. Fitzsimons), Elsevier, Amsterdam, **1973**, p. 263.
[22] T. Peters in *Advances in Protein Chemistry, Vol. 37* (Eds.: C. B. Anfinsen, J. T. Edsall, F. M. Richards), Academic Press, San Diego, **1985**, p. 161.
[23] E. M. Burke, Y. Guo, L. Colon, M. Rahima, A. Veis, G. H. Nancollas, *Colloids Surf. B* **2000**, *17*, 49.
[24] This film can be viewed in the internet under http://www.mpikg-golm.mpg.de/kc/anna/.

  1433-7851/01/4018-3383 $ 17.50+.50/0